JACS
JOURNAL OF THE AMERICAN CHEMICAL SOCIETY

Article

pubs.acs.org/JACS

The N-terminal Region of Amyloid β Controls the Aggregation Rate and Fibril Stability at Low pH Through a Gain of Function Mechanism

Kristoffer Brännström,[†] Anders Öhman,[‡] Lina Nilsson,[∥] Mathias Pihl,[†] Linda Sandblad,[§] and Anders Olofsson*,[†]

[†]Department of Medical Biochemistry and Biophysics, [§]Department of Molecular Biology, and [∥]Department of Chemistry, Umeå University, SE-901 87, Umeå, Sweden

[‡]Department of Pharmacology and Clinical Neuroscience, Umeå University, SE-901 85 Umeå, Sweden

Supporting Information

ABSTRACT: Alzheimer's disease is linked to a pathological polymerization of the endogenous amyloid β-peptide (Aβ) that ultimately forms amyloid plaques within the human brain. We used surface plasmon resonance (SPR) to measure the kinetic properties of Aβ fibril formation under different conditions during the polymerization process. For all polymerization processes, a critical concentration of free monomers, as defined by the dissociation equilibrium constant (K_D), is required for the buildup of the polymer, for example, amyloid fibrils. At concentrations below the K_D, polymerization cannot occur. However, the K_D for Aβ has previously been shown to be several orders of magnitude higher than the concentrations found in the cerebrospinal and interstitial fluids of the human brain, and the mechanism by which Aβ amyloid forms *in vivo* has been a matter of debate. Using SPR, we found that the K_D of Aβ dramatically decreases as a result of lowering the pH. Importantly, this effect enables Aβ to polymerize within a picomolar concentration range that is close to the physiological Aβ concentration within the human brain. The stabilizing effect is dynamic, fully reversible, and notably pronounced within the pH range found within the endosomal and lysosomal pathways. Through sequential truncation, we show that the N-terminal region of Aβ contributes to the enhanced fibrillar stability due to a gain of function mechanism at low pH. Our results present a possible route for amyloid formation at very low Aβ concentrations and raise the question of whether amyloid formation *in vivo* is restricted to a low pH environment. These results have general implications for the development of therapeutic interventions.

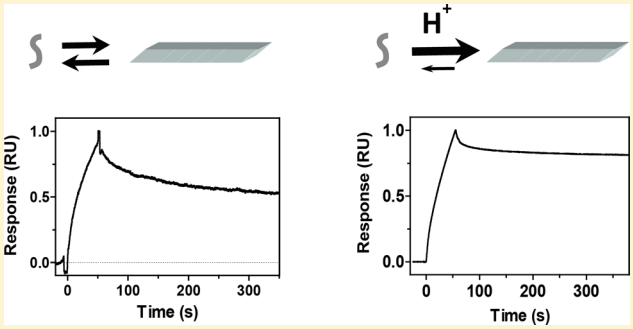

INTRODUCTION

Alzheimer's disease (AD) is by far the most common form of dementia. In 2010, an estimated 36 million individuals were affected by AD around the world, and this figure is predicted to increase due to aging populations.[1] Insoluble amyloid β-peptide (Aβ) fibrils form amyloid plaques within the AD brain, and these are a strong histological hallmark of the disease. The pathology of AD, however, is complicated, and in addition to the formation of extracellular plaques, the disease involves the development of intracellular neurofibrillary tangles and the degeneration of cerebral neurons. Nevertheless, multiple lines of evidence suggest that cytotoxic Aβ assembly is the central and primary event in AD pathogenesis and that the formation of neurofibrillary tangles likely occurs downstream in this cascade.[2,3] Therefore, a detailed understanding of the pathological process of Aβ self-assembly on a molecular level is of fundamental importance to elucidate the factors responsible for the progression of AD and to develop new and effective intervention strategies.

Aβ is derived via sequential proteolytic cleavage of the single transmembrane amyloid precursor protein (APP) by β- and γ-secretases. β-secretase cleaves APP on the intraluminal and extracellular side, and this generates soluble APP and a 99-residue fragment containing Aβ that is still attached to the membrane.[4−8] Aβ is subsequently released by γ-secretase cleavage of the Aβ transmembrane domain.[9,10] This proteolytic excision generates a range of different Aβ variants between 38 and 43 residues in length that exhibit different properties with respect to their ability to self-assemble.[11] The most clinically relevant Aβ variants comprise residues 1−40 ($Aβ_{1-40}$) and 1−42 ($Aβ_{1-42}$).[12] Both $Aβ_{1-40}$ and $Aβ_{1-42}$ can be produced intracellularly, and Aβ might be excised from APP in at least three different locations, including the Golgi apparatus, the endoplasmic reticulum (ER), and the endosomal−lysosomal pathways after re-internalization of surface-exposed APP.[7,8,13]

The exact location of pathological Aβ assembly *in vivo* is unknown, but several cell studies have shown the intracellular formation of Aβ assemblies.[14−17] Extracellular deposits of Aβ plaques are also localized within the vicinity of neuronal cell death and are often seen surrounding dead neurons, which further supports a cellular origin.[18,19]

Received: April 14, 2014
Published: July 11, 2014

   dx.doi.org/10.1021/ja503535m | J. Am. Chem. Soc. 2014, 136, 10956−10964

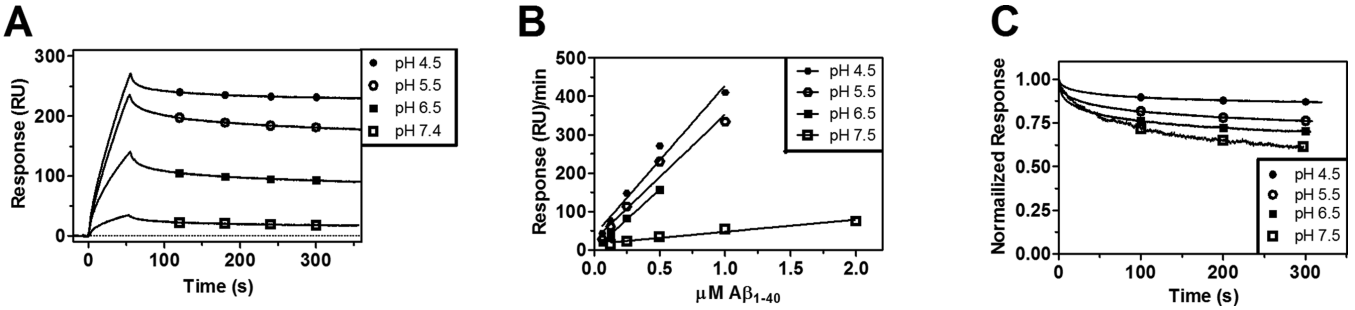

Figure 1. SPR analysis of immobilized Aβ_{1-40} fibrils probed by monomeric Aβ_{1-40} at different pH values. (A) 1 μM Aβ_{1-40} was injected at pH 7.4 (□), pH 6.5 (■), pH 5.5 (○), and pH 4.5 (●). The binding affinity increased with decreasing pH as indicated by the increased response. (B) Increasing concentrations of Aβ_{1-40} were injected over Aβ_{1-40} fibrils at different pH values. The association rate increased with decreasing pH. (C) The normalized response during the dissociation phase after injecting 1 μM Aβ_{1-40} at different pH values. The dissociation rate decreased with decreasing pH.

Analogous to all protein interactions, a critical concentration of free monomers, as defined by the dissociation equilibrium constant (K_D), is required for the formation of amyloid fibrils. At concentrations below the K_D value, polymerization cannot occur. The K_D for Aβ_{1-40} fibrils, which represents the affinity of a monomer to bind to a fibrillar end, has been determined in several independent investigations to be around 100 nM.[20,21] However, the concentration of Aβ found in the cerebrospinal fluid (CSF) is only 50−100 pM. This large discrepancy means that Aβ formation *in vivo* cannot be fully explained. To elucidate the mechanism behind amyloid formation, it is important to identify parameters that either increase the local Aβ concentration or lower the specific K_D.

The intracellular environment might expose Aβ to conditions that significantly differ from the extracellular environment. Perhaps the most notable physical parameter is pH, and a low pH has been associated with more rapid Aβ aggregation.[22−24] The pH within the endosomes and lysosomes *in vivo* is acidic and spans a range from neutral to around pH 5 within the late endosomes[25] and pH 4.5 within the lysosomes.[26] Due to the increased propensity for aggregation at low pH, these compartments have been suggested to be potential sites of Aβ assembly.[27,28] Interestingly, high γ-secretase activity has been found in the lysosomes,[29,30] and accumulation of Aβ_{1-42} within the endosomal−lysosomal system has been shown to appear before plaque deposits in Down syndrome patients who are prone to develop early onset AD.[18,31,32] Modulation of endocytic pathways has been shown to modify the pathological effects of Aβ,[33−36] which is strongly indicative of the important role of the endosomal−lysosomal pathways in self-assembly of Aβ.

Surface plasmon resonance (SPR), in which preformed fibrils are immobilized on a surface and probed by free monomers, can be used to monitor fibrillar assembly.[37−40] This process omits the stochastic nucleation step and enables the rate of fibril formation to be studied in detail. The approach also permits variations in physical conditions as well as cross-seeding experiments between different fibrillar architectures.

In this study, we evaluated the effect of pH on Aβ assembly. Using SPR, we found that lowering the pH induces a very strong stabilizing effect on the fibrils, and we show for the first time how Aβ fibrils might propagate at picomolar concentrations. These results imply that the monomeric Aβ concentrations found in the CSF and interstitial fluids (ISF) are actually rather close to the required K_D for polymerization upon entering the endosomal/lysosomal pathways. We also found that the effect of low pH is dynamic and fully reversible, and through sequential truncation experiments we showed that the stabilizing effect can be attributed to the N-terminal region of the Aβ sequence. These findings provide fundamental insights into the site and formation of Aβ assemblies *in vivo* and have implications for the future design of therapeutic intervention strategies.

RESULTS

Low pH Induces a Dramatic Increase in Aβ_{1-40} Fibril Stability. The binding strength for all protein interactions is defined by the K_D value, which is the ratio of the dissociation rate (k_{off}) and the association rate (k_{on}) and represents the concentration at which 50% of the binding sites are occupied eq 1. For a polymerization process such as amyloid formation, the concentration of free monomers must be above the K_D value for the reaction to occur. The stability of a fibril is, therefore, defined by the affinity of free monomeric Aβ_{1-40} for binding to the fibrillar ends of immobilized Aβ_{1-40}, which is determined by the K_D value.

$$K_D = \frac{k_{off}}{k_{on}} \quad (1)$$

SPR is a very convenient tool to elucidate in detail the different properties of a polymerization process where preformed fibrils can be immobilized on a surface and probed with free monomers. Apart from its very high sensitivity, this approach also circumvents the stochastic nature of nucleation, which precedes the formation of a fibril. In this work, we examined the effect of changes in pH. The pH encountered by the Aβ peptide *in vivo* ranges from 7.4 to 4.5, and we investigated the effect within this specific range. To monitor continuous polymerization, Aβ_{1-40} fibrils were immobilized on the surface of an SPR sensor chip and subsequently probed by free Aβ_{1-40} monomers. The sensograms in Figure 1 show the initial association phase as the fibrils are polymerized followed by the dissociation phase after the injection was stopped.

Due to its intrinsic nature, a polymerization reaction does not reach a point of saturation similar to a ligand−receptor interaction, and the affinity between subunits must be determined through indirect methods. We and others have previously determined that the affinity between subunits, the K_D value, within an Aβ_{1-40} fibril is around 100 nM at neutral pH.[20,21] In this study, the relative change in the rate of polymerization as a function of alterations in the pH is shown, and the affinity constants can be related to this value. Figure 1A

dx.doi.org/10.1021/ja503535m | J. Am. Chem. Soc. 2014, 136, 10956−10964

shows the sensograms at different pH levels with a constant free $A\beta_{1-40}$ monomer concentration of 1 μM. Figure 1B illustrates the association rates of $A\beta_{1-40}$ at different pH values as a function of free $A\beta_{1-40}$ monomer concentration. Interestingly, a significant stabilizing effect was observed after a rather modest reduction in pH. A 10-fold increase in association rate occurred already at pH 6.5, and at pH 4.5 the increase was almost 12 times faster than at neutral pH. Figure 1C shows the normalized dissociation kinetics as a function of pH.

The dissociation phase in Figure 1C follows a biphasic pattern where an initial low affinity, seen as a rapid decay, is followed by a slower rate of dissociation. This process has been previously described as the dock and lock mechanism where the free peptide first attaches to the fibrillar end in a nonoptimal manner with a lower affinity but is subsequently optimized through minor structural changes to adopt a higher affinity conformation that causes the slower rate of dissociation.[41] The contribution to the affinity from the fast decay is minor, and we are, therefore, exclusively focusing only on the high-affinity part where the $A\beta_{1-40}$ monomer has been "locked" into the fibrils and which represents the major part of the dissociation constant. From the results, it is obvious that the low pH dramatically reduces the rate of dissociation. The dissociation rate at pH 6.5 is five times slower than at neutral pH, and the dissociation rate at pH 4.5 is 10.5 times slower. Given the relative changes in association and dissociation kinetics as well as the affinity at one value, the affinity at the different pH values can be calculated. The results are given in Table 1 and show

Table 1. Relative Change in Association and Dissociation Rates of $A\beta_{1\text{-}40}$ at Different pH[a]

pH	relative association rate (k_{on})	1/relative dissociation rate (k_{off})	potentiation	K_D, nM
7.4	1	1	1	100
6.5	10	2	20	5
5.5	10.5	9.5	99	1
4.5	11.8	10.5	124	0.8

[a]All figures are related to the kinetics at neutral pH, which is defined as 1. The K_D between an $A\beta_{1\text{-}40}$ monomer and its fibrillar counterpart at neutral pH is adapted from a recent study.[42]

that at pH 4.5 the binding strength of a monomer within a fibril is 124 times stronger than at neutral pH. The effect is also pronounced upon a modest lowering of the pH and corresponds to a 20-fold increase in affinity already at pH 6.5.

Because of the sometimes strong template-dependent effect of Aβ fibril formation,[21] we investigated whether the $A\beta_{1-40}$ fibrils formed at pH 7.4 and pH 4.5 have the same ability to template a polymerization reaction or if the reaction is somewhat impaired as a result of changes in the environment. We found that the enhanced stability effect is highly dynamic and that the fibrils exhibit an identical ability to template the reaction irrespective of whether they were initially formed at pH 4.5 or 7.4.

The N-Terminal Region of Aβ Controls Fibril Formation Rate and Stability. The experiments described above showed that low pH dramatically influences the aggregation rate by affecting both the dissociation rate and the association rate. However, it was unclear which part of the peptide mediates the stabilizing effect and whether the effect is caused by a protective mechanism at neutral pH or a gain of function at low pH. To investigate this, preformed $A\beta_{1-40}$ fibrils, which preserved the architecture of the template fibril, were probed by N-terminally truncated Aβ variants $A\beta_{3-40}$, $A\beta_{11-40}$, and $A\beta_{17-40}$. The experiment was performed at pH 7.4 and 4.5. For $A\beta_{3-40}$ and $A\beta_{11-40}$, the association rate, which is the rate the monomeric peptides are incorporated into the $A\beta_{1-40}$ fibril, was essentially identical (Figure 2A). Both $A\beta_{3-40}$ and $A\beta_{11-40}$ had the same increase in association rate after lowering the pH from neutral to pH 4.5 as $A\beta_{1-40}$ (Figure 2A,B). $A\beta_{17-40}$ was also incorporated into the architecture of $A\beta_{1-40}$ fibrils, but this variant had a lower pH-mediated increase in the association rate (Figures 2A and 2B). The results suggest that the residues spanning the Glu11-Lys16 region are of particular importance for the rate of association.

Evaluation of the dissociation rates showed that the Asp1-Tyr10 region of the N-terminal region of Aβ also contributes to fibrillar stability. Removing the first two amino acids resulted in an increased rate of dissociation as well as a notably longer docking phase. Figure 2C shows the dissociation response with $A\beta_{1-40}$ at pH 7.4 and pH 4.5, and Figure 2D shows the dissociation response with the $A\beta_{3-40}$ variant at both neutral pH and at pH 4.5. Further truncation, represented by the $A\beta_{11-40}$ variant, had a surprisingly small effect on the dissociation response and showed essentially the same properties as $A\beta_{3-40}$ at pH 4.5 and pH 7.4 as shown in Figure 2E. This indicates a small direct influence by the region spanning Glu3-Tyr10. However, further truncation resulted in a more dramatic change, and probing $A\beta_{1-40}$ fibrils with $A\beta_{17-40}$ monomers showed a pronounced increase in the dissociation rate and, interestingly, a complete loss of the potentiating effect of lowering the pH (Figure 2F). In contrast to the association rate, which is affected by the concentration of the free peptide, the dissociation rate is independent of the concentration. This implies that the influence of the dissociation rate becomes increasingly important at lower concentrations.

Using the $A\beta_{1-40}$ fibrils as a template preserved the uniform architecture that otherwise might have induced a variable component in the system due to the possible formation of alternative fibrillar architectures by the truncated variants. It is, however, interesting to note that repeating all of these experiments using the corresponding fibrils as a template resulted in an identical result, which is shown in Supporting Information Figure S1. The $A\beta_{17-40}$ variant presented technical difficulties when using $A\beta_{17-40}$ fibrils as the template due to the intrinsically high rate of dissociation.

The pH-Dependent Effect Is Not Mediated by a Change in Secondary Structure of Aβ. Aβ is an intrinsically disordered peptide and does not form stable structures in solution at neutral pH. The strong increase in aggregation rate after lowering the pH is puzzling, and from a mechanistic point of view the events preceding incorporation into fibrils are not clear. Several scenarios, however, are possible where either the fibril or the monomeric structure is changed prior to incorporation. Circular dichroism (CD) analysis of the monomer was used to investigate whether the mechanism requires the formation of stable structure within the monomer to facilitate incorporation. The striking effect we observed in the previous experiments after a very small change in pH implies that any potential change should be seen within this pH range. Therefore, the secondary structure of monomeric $A\beta_{1-40}$ was analyzed at pH 7.4, 6.5, and 6.0. The CD spectra at neutral pH indicated predominantly random coil structures, and only very minor changes in secondary structure occurred within this pH range (Figure 3).

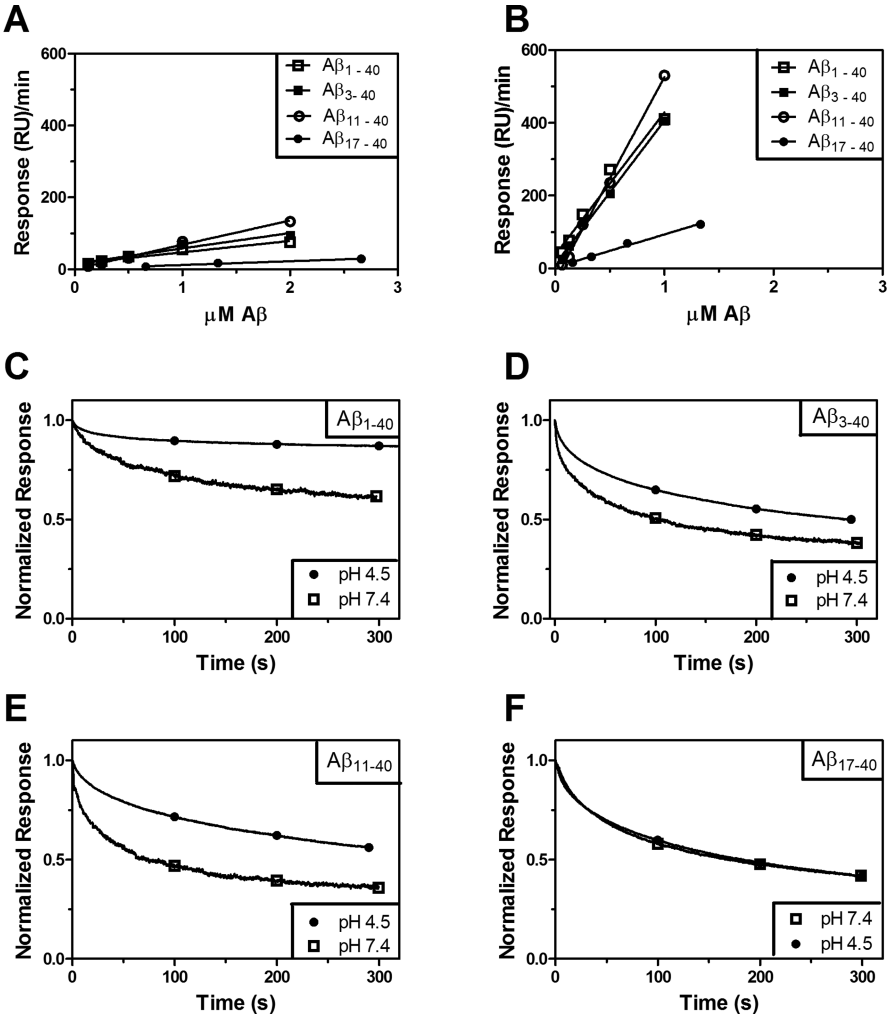

Figure 2. SPR analysis of immobilized Aβ_{1-40} fibrils probed with different monomeric Aβ variants at pH 7.4 and pH 4.5. Association rates monitored as a function of increasing concentrations of Aβ_{1-40}, Aβ_{3-40}, Aβ_{11-40}, and Aβ_{17-40} injected over Aβ_{1-40} fibrils at pH 7.4 (A) and pH 4.5 (B). Dissociation responses after injection of 1 μM Aβ_{1-40} (C), Aβ_{3}-40 (D), Aβ_{11-40} (E), and Aβ_{17-40} (F) at pH 7.4 (■) and pH 4.5 (□).

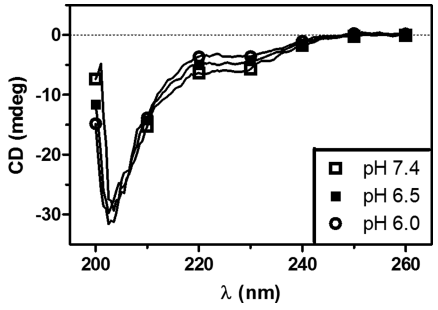

Figure 3. CD of Aβ_{1-40} monomers at different pH values. Aβ_{1-40} samples (10 μM) were analyzed at 25 °C at pH 7.4 (□), pH 6.5 (■), and pH 6.0 (○). Lowering the pH from 7.4 to 6.0 did not affect the secondary structure of Aβ_{1-40}.

Electron Microscopy Indicates a Similar Morphology among Truncated Aβ Variants. Electron microscopy (EM) was used to verify the ability of the investigated Aβ variants to form amyloid structures at both pH 7.4 and 4.5. After incubation, all Aβ variants displayed fibrillar morphologies. Figure 4 shows that Aβ_{1-40} forms fibrils within the pH range 4.5−7.4. The lengths differed somewhat, but the diameters were similar at 10 nm. The fibrillar structures of Aβ_{3-40},

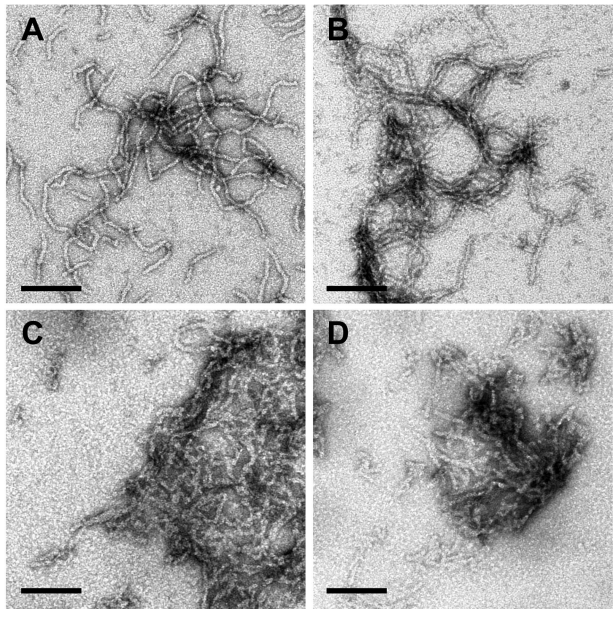

Figure 4. Negative-staining EM of Aβ_{1-40} aggregates verifies fibrillar morphologies at (A) pH 7.4, (B) pH 6.5, (C) pH 5.5, and (D) pH 4.5.

dx.doi.org/10.1021/ja503535m | J. Am. Chem. Soc. 2014, 136, 10956−10964

$A\beta_{11-40}$, and $A\beta_{17-40}$ at both neutral and low pH were also verified using EM and are shown in Supporting Information Figure S2.

Quenched H/D Exchange Experiments. The dramatic increase in polymerization kinetics at low pH indicates differences in the ability of the fibrils to act as templates for $A\beta$ polymerization. This could have several different explanations. We used quenched hydrogen/deuterium (H/D) exchange in combination with NMR according to a previously established procedure[42,43] to evaluate the possibility of changes in the core structure of the fibrils. The method is based on the rationale that the secondary structure in the fibrillar core protects the labile amide protons from exchanging with the surrounding deuterons. After a defined time of incubation in D_2O, the solvent protection is trapped via a rapid conversion of the fibrils into a monomeric and NMR-detectable state during conditions of low back exchange. By monitoring the post-trap decay of the H/D exchange, the method identifies the fibrillar core in a residue-specific and quantitative manner. Using this approach, we found that the solvent-protected core structure was essentially identical for fibrils formed at pH 7.4, 6.5, and 5.0 (Figure 5). These fibrils displayed two well-protected bell-shaped regions spanning Ser9-Gly25 and Gly27-Val40 and a less protected region centered on residue Ser26, which is consistent with a structural arrangement of two β-strands connected by a turn and is in agreement with a current solid-state NMR model.[42]

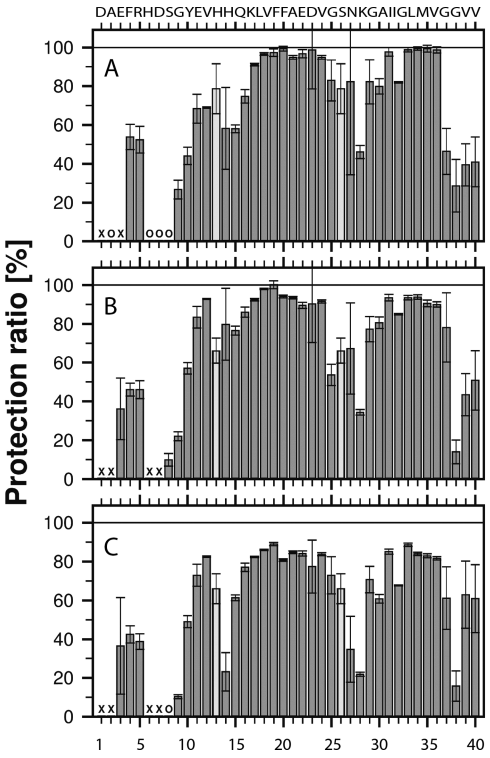

Figure 5. Solvent protection ratios for backbone amide protons as determined by quenched H/D exchange monitored by NMR spectroscopy. The plots show solvent protection patterns from fibrils formed at pH 7.5 (A), pH 6.5 (B), and pH 5.0 (C). Protection is defined as the ratio of the observed signal intensity after a given time of preincubation in D_2O compared to a completely protonated reference sample. Protection in the reference sample is defined as 100%. Circles correspond to residues verified to have 0% protection, and crosses correspond to residues where exchange was too fast for detection. Pale gray bars indicate overlapping residues with ambiguously assigned protection ratios. Error bars indicate the experimental uncertainty.

DISCUSSION

The equilibrium between monomeric $A\beta$ peptides and their pathological self-assembly is delicate, and it is well-known that just a small perturbation could have devastating effects and result in early onset AD. Factors such as $A\beta$ expression levels,[44,45] secretase excision efficiency,[46,47] ApoE genotype,[48] and differential trafficking within the endosomal−lysosomal pathways[49] are just a few examples of factors known to contribute to the risk of developing the disease. Elucidation of the parameters affecting these equilibriums is important in order to fully understand the pathology of AD.

The polymerization of an amyloid fibril can be regarded as the formation of a one-dimensional crystal where a template-dependent mechanism controls both the ability to polymerize as well as the rate of fibril formation. With SPR, it is possible to obtain the rate constants of the polymerization process without having to account for the stochastic phase of nucleation.[37,38] This allows the properties of the template and substrate to be evaluated as well as the effects of environmental factors.

All polymerization processes, however, depend on a critical concentration to occur. This concentration is defined as the dissociation equilibrium constant, K_D. At a monomeric concentration below the K_D the dissociated state is more favorable and polymerization will not occur. Therefore, the concentration of $A\beta$ is important and determines whether a fibril will form or not.

The critical concentration for $A\beta_{1-40}$ at neutral pH has been previously determined, both by us and by others, to be around 100 nM.[20,21] However, the concentration of $A\beta$ within the CSF is only 50−100 pM,[50] which means that the extracellular concentration of free $A\beta$ is approximately 1000−2000 times lower than the concentration required for the polymerization process to occur. Although self-assembly of $A\beta$ has been shown to be promoted, for example, by binding to membranes,[51,52] this large discrepancy raises questions about how and where polymerization of $A\beta$ might occur. In this study, we found that lowering the pH to the values found in endosomes and lysosomes dramatically lowered the K_D, which for the first time shows that $A\beta$ fibril formation can occur within the picomolar range.

The stabilizing effect as a function of pH is clearly dependent on the ionizable groups of the peptide that determine the isoelectric point (PI) and hydrophobicity and, therefore, the overall solubility. Full-length $A\beta$ is an amphipathic peptide with both a charged part and a predominantly hydrophobic part. Most of the charged residues are located within the N-terminal region of residues Asp1-Lys16, and the C-terminal stretch is mainly hydrophobic. For illustrative purposes, Figure 6 shows a hydrophobicity plot where the charged residues have been indicated within the sequence. The degree of protonation of the specific ionizable groups on the peptide, including the peptide N-terminus and the side-chains of Arg, Lys, His, Glu, and Asp, is dependent on their specific pK_a values. The side-chains of Arg and Lys both have alkaline pK_a values corresponding to 12.5 and 10, respectively, and both will have a positive charge for all pH values in the current investigation. The pK_a values for Asp, Glu, and His have previously been specifically determined within the $A\beta$ peptide and correspond to around 4.2, 4.3, and 6.2, respectively.[53] The observed strong stabilizing effect at a

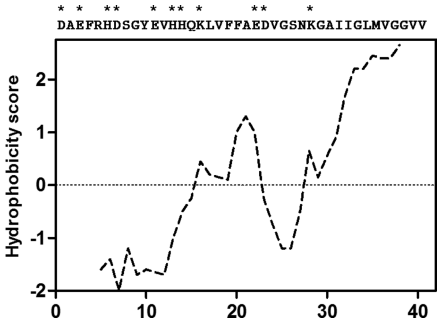

Figure 6. Sequence analysis of Aβ_{1-40} using the Kyle and Doolittle algorithm for predicting hydrophobicity. Charged residues (*) are indicated in the sequence.

pH just below neutral implies that the predominant effect is the result of protonation of the histidines and possibly the N-terminus, which has a pK_a around 7.0. The results showed that a nearly full effect of stabilization is reached at pH 5.5. At this pH, essentially all of the histidines are protonated but only a very small proportion of the carboxyl groups on Asp and Glu are protonated.

To identify the mechanism associated with the pH-dependent stabilization, we investigated the effect as a function of sequential truncations of the N-terminal region of the peptide. We found that removal of only the first two residues had a surprisingly strong influence on both fibrillar stability and the pH-dependent potentiation, which shows that the absolute N-terminal part significantly contributes to the fibrillar stability. Although it is difficult to pinpoint the exact mechanism because the truncation both removes a negative charge due to removal of Asp1 and shifts the location of the N-terminus, the effect is notable and implies that the Aβ_{3-40} variants, which are abundant *in vivo*,[6,54] will display a different stability compared to Aβ_{1-40}.

Addition or removal of charged residues might have an effect on the overall solubility of the peptide, and increased water solubility would favor a monomeric state. In this context it is important to consider potential changes in PI that might influence the equilibrium due to changed solubility at the specific pH. Table 2 lists the PI, hydrophobicity, and overall charge as well as the change in charge within the investigated pH range.

Removal of the two initial residues only shifts the PI from 5.31 to 5.71 and, therefore, cannot explain the reduced fibril stability. The overall hydrophobicity also increases slightly because of the truncation, which would favor rather than weaken the interaction due to the lower water solubility, and this cannot explain the decreased stability either. Further truncation by removal of the first 10 N-terminal residues, on the contrary, had a surprisingly small effect, and Aβ_{11-40} had essentially the same properties as Aβ_{3-40}, which indicates that Glu3-Tyr10 is not significantly involved in the overall stability of the fibril or the pH-dependent mechanism of fibril stabilization. It is of particular interest to note that protonation of His6 does not seem to make a significant contribution to the observed effect. Aβ_{11-40} has a PI of 6.02, which is in the same range as Aβ_{3-40}, but the hydrophobicity index is increased even further.

Truncating the peptide further by removing residues Glu11–Lys16 had a much more striking effect. Probing Aβ_{1-40} fibrils with monomeric Aβ_{17-40} produced a less stable fibril and, importantly, no stabilizing effect resulted from lowering the pH. This result is in accordance with the notion that no significant change in charge can be seen within the specific pH range. The PI of Aβ_{17-40} is 6.07 and is in the same range as the PIs of longer Aβ variants. However, due to removal of the hydrophilic N-terminal part the remaining sequence is highly hydrophobic. Nevertheless, the binding affinity toward the fibrillar end is significantly diminished.

Although we found an H/D protection pattern that indicates contacts within the fibrillar structure, molecular explanations for the affinity at which a peptide binds to a fibrillar end should be treated with care. The H/D protection pattern represents the ability of the structure to protect the labile amide hydrogen from reacting with water. This can be achieved either through formation of a hydrogen bond within the secondary structure or via solvent exclusion of hydrophobic areas due to the fibrillar architecture. Truncation of the first two residues resulted in a significantly lower stability. This could possibly be attributed to the proximity to, and interference with, the protected residues Glu3–Arg5, which are likely protected through hydrogen bonds because this is a rather hydrophilic peptide stretch of the peptide. The similar stability between Aβ_{3-40} and Aβ_{11-40}, where the latter lacks the ability to make stabilizing contacts within the 10 most N-terminal residues, is hard to explain and pinpoints the difficulty of determining the stability based only on the relative solvent exclusion. According to these results, the stretch between Glu3 and Tyr10 apparently only contributes enough to maintain its own binding and does not significantly contribute to the overall stability of the peptide. It is, however, possible that the two most N-terminal residues are important for the stability of the first 10 residues and function like a zipper for the region, and this would explain our results.

In all experiments, we maintained physiological ionic strength. However, in SPR analysis where salt was omitted we found a less potentiated increase in fibril stability upon lowering the pH, and this suggests that shielding of some charged residues is required. It should also be noted that the effect of stabilizing charge interactions could not be seen in the H/D exchange experiments.

It is, at this point, of interest to present a mechanistic explanation for the observed phenomenon. The reduction in fibril stability by removing the N-terminal region of Aβ could

Table 2

peptide	isoelectric point	hydrophobicity	charge (pH 4.5)	charge (pH 5.5)	charge (pH 7.4)
Aβ1–40	5.31	0.0575	2.2	−0.4	−3.4
Aβ3–40	5.71	0.105	2.9	0.6	−2.4
Aβ11–40	6.02	0.613	2.2	0.7	−1.4
Aβ17–40	6.07	1.312	−0.2	−0.9	−1.5

Isoelectric point was calculated according to Bjellqvist et al., 1994 (ref 55). The hydrophobicity was calculated using the GRAVY algorithm.[56] The number of charges at a specific pH was acquired using the online protein calculator v3.4, http://protcalc.sourceforge.net/.

be explained either by the loss of a protective function at neutral pH or by a gain of function due to the low pH. Considering the possibility of a protective function by the N-terminal region at neutral pH, a truncation would increase the fibril stability. This effect, however, was not observed, and this implies that the N-terminal region of the full-length Aβ peptide gains a function at low pH that facilitates a more rapid incorporation of monomers into the fibrillar architecture. At present, it is not possible to determine the structural changes in detail. It is notable, however, that a rather strong effect occurs already at around pH 6.0−6.5. CD analysis of the monomer in this pH range indicated only minor structural changes, which leads to the conclusion that a substantial structural change, prior to fibril incorporation, is not a prerequisite.

We also could not demonstrate any significant changes in the fibrillar form, and the structural analysis of the fibrils using H/D exchange in combination with NMR did not indicate any considerable difference between fibrils formed at pH 7.4 and 6.5 or even pH 5.0. A substantial structural change in the fibril due to pH shifts is also unlikely to occur due to high kinetic barriers, and this would not fit with the observed dynamic behavior in these experiments. Therefore, the enhancing effect is most likely mediated by changes within the charge interactions of the side chains that were not obvious in the CD or H/D exchange patterns. A possible explanation, therefore, is that a predominantly unstructured monomer adapts the fibrillar structure through an induced fit mechanism. Such a model is in good agreement with the dock and lock mechanism noted within these experiments as well as in several previous investigations.[41,42] An interesting possibility, although speculative, is that protonation of one or more specific histidines enables intramolecular charge interactions resulting in the formation of an aggregation-prone intermediate. Such a conformational change would not necessarily be seen within a CD spectrum. Here it should be mentioned that a previous study aimed at identifying salt-bridge interactions between histidines and carboxyl groups within the Aβ peptide indicated that no intramolecular interactions could be seen within the monomer.[53]

The high template dependency of Aβ fibril assembly is interesting and reflects how very small alterations, such as a change of charge, might have a profound impact on fibril assembly. In this context, it is important to highlight that because only $A\beta_{1-40}$ fibrils were used as a template, the fibrillar architecture was uniform between all experiments. However, using the corresponding fibrils of $A\beta_{3-40}$ as well as $A\beta_{11-40}$ as a template produced very similar results (Supporting Information Figure S1). A detailed analysis of immobilized $A\beta_{17-40}$ fibrils was, as expected, partly impaired because of its high dissociation rate.

The dramatic lowering of the K_D as a result of low pH in this work shows for the first time how a polymerization of Aβ can occur at picomolar concentrations very close to the concentration found in the CSF and the ISF.[57] The actual monomeric Aβ concentration within the endosomes and lysosomes might, however, be higher because APP processing, apart from the Golgi and ER,[58−61] also occurs within the endosomal and lysosomal pathways,[8] which consequently will contribute to an increased local concentration within these compartments. Another factor that could also possibly increase the Aβ concentration within the endosomal and lysosomal compartments is that Aβ has an affinity for certain cell membranes and receptors that could lead to an increased Aβ concentration on the cell surface and, as a consequence, a higher local concentration upon endocytosis. In particular, the interaction between Aβ and the ganglioside GM1 has been studied, and a connection between endocytosis and fibril formation has been suggested.[62] Also, alterations in cholesterol content are known to modify Aβ binding to membranes and to be risk factors for AD.[63] Interestingly a specific Aβ uptake from the extracellular environment resulting in an increased endosomal and lysosomal concentration has also been noted in certain cells.[64]

The present work was exclusively performed with the $A\beta_{1-40}$ variant, but in a previous study we showed that the significantly more aggregation-prone $A\beta_{1-42}$ form is around 10 times more stable than $A\beta_{1-40}$ at neutral pH.[42] The $A\beta_{1-42}$, on the contrary, is found in lower concentrations than $A\beta_{1-40}$, which counteracts this effect.

This work was also exclusively performed with fibrillar structures, but Aβ also has the ability to adopt a range of different structures including highly cytotoxic protofibrillar and oligomeric forms.[39,65] The optimal conditions for the formation of these nonfibrillar assemblies and the critical concentration for their formation should be studied further.

In this study, we have shown how the critical concentration of Aβ fibril assembly dramatically decreases as a result of lowering the pH and that it is possible for Aβ to polymerize within a picomolar concentration range that is close to the Aβ concentration found within the CSF and ISF. We demonstrated how the enhancing effect is mediated by the N-terminal region of Aβ, which acts through a gain of function mechanism at low pH, and how the stabilizing effect essentially correlates with the pK_a of the histidines. We have shown that the effect of pH is highly dynamic, that the increased stability is not associated with a subsequent change in secondary structure of the monomer, and that no significant structural changes are noted for the fibrillar form. These results also raise the question of whether other factors than low pH might decrease the K_D, or increase the Aβ concentration, to cause the same dramatic increase in fibril stability or if the endosomal and lysosomal compartments are, in fact, the exclusive sites where Aβ fibrils can propagate *in vivo*.

MATERIALS AND METHODS

Preparation of Peptides and Fibrillar Samples. Aβ peptides, including isotope-labeled variants, were obtained from AlexoTech AB (Umeå, Sweden). All peptides were solubilized in 10 mM NaOH to an approximate pH of 11, and then the pH was adjusted using phosphate or acetate buffer. All experiments were performed in the presence of 150 mM NaCl unless otherwise indicated. Fibrillar forms were prepared with 100 μM peptide solutions at 37 °C with agitation for 48−96 h.

Negative Staining Electron Microscopy. From each 100 μM Aβ solution, 3.5 μL samples were adsorbed for 2 min onto glow-discharged carbon-coated copper grids, washed in H_2O, and immediately negatively stained in 50 μL of 1.5% uranyl acetate solution for 30 s. Negative-stained samples were examined on a JEM1230 transmission electron microscope (JEOL) operating at 80 kV. Micrographs were recorded with a Gatan UltraScan 1000 2k × 2k pixel CCD camera using Digital Micrograph software.

Surface Plasmon Resonance (SPR). The fibrillar forms of Aβ peptides were immobilized on a CM5 chip (GE Healthcare, Uppsala, Sweden) at a density of around 3000 response units (RU) using standard amine-coupling chemistry. Analysis of Aβ peptide binding was performed using a Biacore 3000 system (GE Healthcare, Uppsala, Sweden) at a flow rate of 20 μL/min in either phosphate buffer (pH between 7.4 and 6.0) or acetate buffer (for analysis at pH 4.5 and pH

5.5). Nonspecific interactions were corrected by using double referencing according to standard procedures.[66] The decay of the Aβ fibrils was fitted to a second-order exponential model, $Ae^{-k_{fast}} + Be^{-k_{slow}} + C$, where the parameters A and B are the percentages of k_{fast} and k_{slow}, respectively. C is a constant required for an optimal fit and represents the fraction of the material that does not dissociate from the template over a very long time scale (<10%).

Quenched H/D Exchange and NMR Analysis of $A\beta_{1-40}$. To evaluate the effect of low pH on fibrillar amyloid, ^{15}N-labeled $A\beta_{1-40}$ (100 μM) was dissolved as described above and incubated under agitation at 37 °C in PBS or acetate buffer over 4 days. To probe solvent accessibility, fibrillar solutions of each peptide type were split into two fractions and recovered by brief centrifugation (20,000× g). H/D exchange was carried out on one of the fractions by diluting the pellets 30 times using a D_2O solution containing 150 mM NaCl and either 20 mM phosphate buffer at pH 7.4 or acetate/acetic acid at pH 4.5. The amide hydrogen exchange rate is logarithmically dependent on pH, so the time of exchange was extended to account for this. At neutral pH, the fibrils were incubated in the deuterated solvent for 1 h, but the exchange at pH 4.5 was prolonged accordingly. (It was, however, apparent that the solvent exchange pattern was mostly dependent on the secondary structure because variations in preincubation times only had a minor influence on the resulting solvent H/D protection pattern.) The second fraction was used as a fully protonated reference sample to identify and exclude amide exchange resulting from the experimental procedure, for example, the exchange of highly exposed amides in the monomeric state. At the end of the incubation period in the deuterated solvent and immediately prior to NMR analysis, Aβ assemblies were recovered by centrifugation and converted into an NMR-detectable state according to a previously described procedure.[67−70] Hydrogen exchange was subsequently monitored by recording a series of heteronuclear 2D ^{15}N-HSQC experiments. Prior to each ^{15}N-HSQC experiment, a 1D proton NMR spectrum was acquired to quantitatively monitor the dissolution of fibrils into monomers. All experiments were performed at 15 °C with a 600 MHz Bruker AVANCE spectrometer equipped with a 5 mm triple-resonance, pulsed-field z-gradient cryoprobe. All spectra were processed using NMRPipe,[71] and spectral analyses were performed in NMRView.[72] The ratios of peak intensities between the different experiments were presented in a residue-specific manner using the Grace software package (plasma-gate.weizmann.ac.il/Grace).

Circular Dichroism. CD spectra were acquired using a Jasco-720 instrument. The spectra between 200 and 260 nm were recorded by collecting data at 0.5 nm intervals with a response time of 2 s and a scan speed of 50 nm/min. Measurements were performed at 20 °C in a 1 cm cuvette in 20 mM phosphate buffer at pH 7.4, 6.5, and 6.0 with 150 mM NaF and 10 μM $A\beta_{1-40}$.

■ ASSOCIATED CONTENT

Supporting Information

An SPR analysis showing the polymerization process of $A\beta_{3-40}$ and $A\beta_{11-40}$ using their corresponding fibrils as a template as well as a TEM analysis of the morphology. This material is available free of charge via the Internet at http://pubs.acs.org.

■ AUTHOR INFORMATION

Corresponding Author

anders.olofsson@medchem.umu.se

Notes

The authors declare no competing financial interest.

■ ACKNOWLEDGMENTS

Funding for this work was provided by the Erling-Persson Family Foundation, Parkinsonfonden, Insamlingsstiftelsen Umeå University, Alzheimerfonden, J.C. Kempe, the Swedish Research Council, Magn. Bergvalls stiftelse, O.E. och Edlas stiftelse, Torsten Söderbergs stiftelse, Västerbottens Läns landsting (ALF-medel), FAMY, and the Medical Faculty of Umeå University.

■ REFERENCES

(1) Prince, M.; Bryce, R.; Albanese, E.; Wimo, A.; Ribeiro, W.; Ferri, C. P. *Alzheimer's Dementia* **2013**, *9*, 63.
(2) Hardy, J.; Selkoe, D. J. *Science* **2002**, *297*, 353.
(3) Caccamo, A.; Oddo, S.; Sugarman, M. C.; Akbari, Y.; LaFerla, F. M. *Neurobiol. Aging* **2005**, *26*, 645.
(4) Bien, J.; Jefferson, T.; Causevic, M.; Jumpertz, T.; Munter, L.; Multhaup, G.; Weggen, S.; Becker-Pauly, C.; Pietrzik, C. U. *J. Biol. Chem.* **2012**, *287*, 33304.
(5) Sambamurti, K.; Shioi, J.; Anderson, J. P.; Pappolla, M. A.; Robakis, N. K. *J. Neurosci. Res.* **1992**, *33*, 319.
(6) Valenti, M. T.; Bolognin, S.; Zanatta, C.; Donatelli, L.; Innamorati, G.; Pampanin, M.; Zanusso, G.; Zatta, P.; Dalle Carbonare, L. *J. Alzheimer's Dis.* **2013**, *34*, 263.
(7) Haass, C.; Hung, A. Y.; Selkoe, D. J.; Teplow, D. B. *J. Biol. Chem.* **1994**, *269*, 17741.
(8) Bustamante, H. A.; Rivera-Dictter, A.; Cavieres, V. A.; Munoz, V. C.; Gonzalez, A.; Lin, Y.; Mardones, G. A.; Burgos, P. V. *PloS One* **2013**, *8*, e83096.
(9) Tomita, T.; Iwatsubo, T. *J. Biol. Chem.* **2013**, *288*, 14673.
(10) Evin, G.; Cappai, R.; Li, Q. X.; Culvenor, J. G.; Small, D. H.; Beyreuther, K.; Masters, C. L. *Biochemistry* **1995**, *34*, 14185.
(11) Qi-Takahara, Y.; Morishima-Kawashima, M.; Tanimura, Y.; Dolios, G.; Hirotani, N.; Horikoshi, Y.; Kametani, F.; Maeda, M.; Saido, T. C.; Wang, R.; Ihara, Y. *J. Neurosci.* **2005**, *25*, 436.
(12) Masters, C. L.; Simms, G.; Weinman, N. A.; Multhaup, G.; McDonald, B. L.; Beyreuther, K. *Proc. Natl. Acad. Sci. U.S.A.* **1985**, *82*, 4245.
(13) Wertkin, A. M.; Turner, R. S.; Pleasure, S. J.; Golde, T. E.; Younkin, S. G.; Trojanowski, J. Q.; Lee, V. M. *Proc. Natl. Acad. Sci. U.S.A.* **1993**, *90*, 9513.
(14) Turner, R. S.; Suzuki, N.; Chyung, A. S.; Younkin, S. G.; Lee, V. M. *J. Biol. Chem.* **1996**, *271*, 8966.
(15) Martin, B. L.; Schrader-Fischer, G.; Busciglio, J.; Duke, M.; Paganetti, P.; Yankner, B. A. *J. Biol. Chem.* **1995**, *270*, 26727.
(16) Walsh, D. M.; Tseng, B. P.; Rydel, R. E.; Podlisny, M. B.; Selkoe, D. J. *Biochemistry* **2000**, *39*, 10831.
(17) Kulic, L.; McAfoose, J.; Welt, T.; Tackenberg, C.; Spani, C.; Wirth, F.; Finder, V.; Konietzko, U.; Giese, M.; Eckert, A.; Noriaki, K.; Shimizu, T.; Murakami, K.; Irie, K.; Rasool, S.; Glabe, C.; Hock, C.; Nitsch, R. M. *Transl. Psychiatry* **2012**, *2*, e183.
(18) Gouras, G. K.; Tsai, J.; Naslund, J.; Vincent, B.; Edgar, M.; Checler, F.; Greenfield, J. P.; Haroutunian, V.; Buxbaum, J. D.; Xu, H.; Greengard, P.; Relkin, N. R. *Am. J. Pathol.* **2000**, *156*, 15.
(19) D'Andrea, M. R.; Nagele, R. G. *Biotech. Histochem.* **2010**, *85*, 133.
(20) Aguilar, M. I.; Small, D. H. *Neurotoxic. Res.* **2005**, *7*, 17.
(21) Brannstrom, K.; Ohman, A.; Olofsson, A. *PloS One* **2011**, *6*, e25157.
(22) Su, Y.; Chang, P. T. *Brain Res.* **2001**, *893*, 287.
(23) Burdick, D.; Soreghan, B.; Kwon, M.; Kosmoski, J.; Knauer, M.; Henschen, A.; Yates, J.; Cotman, C.; Glabe, C. *J. Biol. Chem.* **1992**, *267*, 546.
(24) McAllister, C.; Karymov, M. A.; Kawano, Y.; Lushnikov, A. Y.; Mikheikin, A.; Uversky, V. N.; Lyubchenko, Y. L. *J. Mol. Biol.* **2005**, *354*, 1028.
(25) Cain, C. C.; Sipe, D. M.; Murphy, R. F. *Proc. Natl. Acad. Sci. U.S.A.* **1989**, *86*, 544.
(26) Mellman, I.; Fuchs, R.; Helenius, A. *Annu. Rev. Biochem.* **1986**, *55*, 663.
(27) Annunziata, I.; Patterson, A.; Helton, D.; Hu, H.; Moshiach, S.; Gomero, E.; Nixon, R.; d'Azzo, A. *Nat. Commun.* **2013**, *4*, 2734.
(28) Tam, J. H.; Pasternak, S. H. *Can. J. Neurol. Sci.* **2012**, *39*, 286.
(29) Pasternak, S. H.; Bagshaw, R. D.; Guiral, M.; Zhang, S.; Ackerley, C. A.; Pak, B. J.; Callahan, J. W.; Mahuran, D. J. *J. Biol. Chem.* **2003**, *278*, 26687.

(30) Bagshaw, R. D.; Pasternak, S. H.; Mahuran, D. J.; Callahan, J. W. *Biochem. Biophys. Res. Commun.* **2003**, *300*, 615.
(31) Gyure, K. A.; Durham, R.; Stewart, W. F.; Smialek, J. E.; Troncoso, J. C. *Arch. Pathol. Lab. Med.* **2001**, *125*, 489.
(32) Cataldo, A. M.; Petanceska, S.; Terio, N. B.; Peterhoff, C. M.; Durham, R.; Mercken, M.; Mehta, P. D.; Buxbaum, J.; Haroutunian, V.; Nixon, R. A. *Neurobiol. Aging* **2004**, *25*, 1263.
(33) Treusch, S.; Hamamichi, S.; Goodman, J. L.; Matlack, K. E.; Chung, C. Y.; Baru, V.; Shulman, J. M.; Parrado, A.; Bevis, B. J.; Valastyan, J. S.; Han, H.; Lindhagen-Persson, M.; Reiman, E. M.; Evans, D. A.; Bennett, D. A.; Olofsson, A.; DeJager, P. L.; Tanzi, R. E.; Caldwell, K. A.; Caldwell, G. A.; Lindquist, S. *Science* **2011**, *334*, 1241.
(34) Abramowski, D.; Rabe, S.; Upadhaya, A. R.; Reichwald, J.; Danner, S.; Staab, D.; Capetillo-Zarate, E.; Yamaguchi, H.; Saido, T. C.; Wiederhold, K. H.; Thal, D. R.; Staufenbiel, M. *J. Neurosci.* **2012**, *32*, 1273.
(35) Butler, D.; Hwang, J.; Estick, C.; Nishiyama, A.; Kumar, S. S.; Baveghems, C.; Young-Oxendine, H. B.; Wisniewski, M. L.; Charalambides, A.; Bahr, B. A. *PloS One* **2011**, *6*, e20501.
(36) Zheng, L.; Calvo-Garrido, J.; Hallbeck, M.; Hultenby, K.; Marcusson, J.; Cedazo-Minguez, A.; Terman, A. *J. Alzheimer's Dis.* **2013**, *37*, 713.
(37) Cannon, M. J.; Williams, A. D.; Wetzel, R.; Myszka, D. G. *Anal. Biochem.* **2004**, *328*, 67.
(38) Hasegawa, K.; Ono, K.; Yamada, M.; Naiki, H. *Biochemistry* **2002**, *41*, 13489.
(39) Qiang, W.; Kelley, K.; Tycko, R. *J. Am. Chem. Soc.* **2013**, *135*, 6860.
(40) Hou, X.; Small, D. H.; Aguilar, M. I. *Methods Mol. Biol.* **2010**, *627*, 225.
(41) Esler, W. P.; Stimson, E. R.; Jennings, J. M.; Vinters, H. V.; Ghilardi, J. R.; Lee, J. P.; Mantyh, P. W.; Maggio, J. E. *Biochemistry* **2000**, *39*, 6288.
(42) Brannstrom, K.; Ohman, A.; Lindhagen-Persson, M.; Olofsson, A. *Biochem. J.* **2013**, *450*, 189.
(43) Olofsson, A.; Lindhagen-Persson, M.; Sauer-Eriksson, A. E.; Ohman, A. *Biochem. J.* **2007**, *404*, 63.
(44) Lahiri, D. K.; Ge, Y. W. *Ann. N.Y. Acad. Sci.* **2004**, *1030*, 310.
(45) Schupf, N.; Patel, B.; Pang, D.; Zigman, W. B.; Silverman, W.; Mehta, P. D.; Mayeux, R. *Arch. Neurol.* **2007**, *64*, 1007.
(46) Winkler, E.; Kamp, F.; Scheuring, J.; Ebke, A.; Fukumori, A.; Steiner, H. *J. Biol. Chem.* **2012**, *287*, 21326.
(47) Kang, E. L.; Biscaro, B.; Piazza, F.; Tesco, G. *J. Biol. Chem.* **2012**, *287*, 42867.
(48) Tai, L. M.; Bilousova, T.; Jungbauer, L.; Roeske, S. K.; Youmans, K. L.; Yu, C.; Poon, W. W.; Cornwell, L. B.; Miller, C. A.; Vinters, H. V.; Van Eldik, L. J.; Fardo, D. W.; Estus, S.; Bu, G.; Gylys, K. H.; Ladu, M. J. *J. Biol. Chem.* **2013**, *288*, 5914.
(49) Li, J.; Kanekiyo, T.; Shinohara, M.; Zhang, Y.; LaDu, M. J.; Xu, H.; Bu, G. *J. Biol. Chem.* **2012**, *287*, 44593.
(50) Rosen, C.; Andreasson, U.; Mattsson, N.; Marcusson, J.; Minthon, L.; Andreasen, N.; Blennow, K.; Zetterberg, H. *Neuromolecular medicine* **2012**, *14*, 65.
(51) Sabate, R.; Espargaro, A.; Barbosa-Barros, L.; Ventura, S.; Estelrich, J. *Biochimie* **2012**, *94*, 1730.
(52) Nagarathinam, A.; Hoflinger, P.; Buhler, A.; Schafer, C.; McGovern, G.; Jeffrey, M.; Staufenbiel, M.; Jucker, M.; Baumann, F. *J. Neurosci.* **2013**, *33*, 19284.
(53) Zhang, S.; Lee, J. P. *J. Pept. Res.* **2000**, *55*, 1.
(54) Drew, S. C.; Masters, C. L.; Barnham, K. J. *J. Am. Chem. Soc.* **2009**, *131*, 8760.
(55) Bjellqvist, B.; Basse, B.; Olsen, E.; Celis, J. E. *Electrophoresis* **1994**, *15*, 529.
(56) Gasteiger, E.; Gattiker, A.; Hoogland, C.; Ivanyi, I.; Appel, R. D.; Bairoch, A. *Nucleic Acids Res.* **2003**, *31*, 3784.
(57) Brody, D. L.; Magnoni, S.; Schwetye, K. E.; Spinner, M. L.; Esparza, T. J.; Stocchetti, N.; Zipfel, G. J.; Holtzman, D. M. *Science* **2008**, *321*, 1221.
(58) Hartmann, T.; Bieger, S. C.; Bruhl, B.; Tienari, P. J.; Ida, N.; Allsop, D.; Roberts, G. W.; Masters, C. L.; Dotti, C. G.; Unsicker, K.; Beyreuther, K. *Nat. Med.* **1997**, *3*, 1016.
(59) Wild-Bode, C.; Yamazaki, T.; Capell, A.; Leimer, U.; Steiner, H.; Ihara, Y.; Haass, C. *J. Biol. Chem.* **1997**, *272*, 16085.
(60) Cook, D. G.; Forman, M. S.; Sung, J. C.; Leight, S.; Kolson, D. L.; Iwatsubo, T.; Lee, V. M.; Doms, R. W. *Nat. Med.* **1997**, *3*, 1021.
(61) Xia, W.; Zhang, J.; Ostaszewski, B. L.; Kimberly, W. T.; Seubert, P.; Koo, E. H.; Shen, J.; Selkoe, D. J. *Biochemistry* **1998**, *37*, 16465.
(62) Yuyama, K.; Yanagisawa, K. *Neurosci. Lett.* **2010**, *481*, 168.
(63) Verdier, Y.; Zarandi, M.; Penke, B. *J. Pept. Sci.* **2004**, *10*, 229.
(64) Hu, X.; Crick, S. L.; Bu, G.; Frieden, C.; Pappu, R. V.; Lee, J. M. *Proc. Natl. Acad. Sci. U.S.A.* **2009**, *106*, 20324.
(65) Pham, J. D.; Chim, N.; Goulding, C. W.; Nowick, J. S. *J. Am. Chem. Soc.* **2013**, *135*, 12460.
(66) Myszka, D. G. *J. Mol. Recognit.* **1999**, *12*, 279.
(67) Olofsson, A.; Lindhagen-Persson, M.; Sauer-Eriksson, A. E.; Ohman, A. *Biochem. J.* **2007**, *404*, 63−70.
(68) Ippel, J. H.; Olofsson, A.; Schleucher, J.; Lundgren, E.; Wijmenga, S. S. *Proc. Natl. Acad. Sci. U.S.A.* **2002**, *99*, 8648.
(69) Olofsson, A.; Lindhagen-Persson, M.; Vestling, M.; Sauer-Eriksson, A. E.; Ohman, A. *FEBS J.* **2009**, *276*, 4051.
(70) Olofsson, A.; Sauer-Eriksson, A. E.; Ohman, A. *Anal. Biochem.* **2009**, *385*, 374.
(71) Delaglio, F.; Grzesiek, S.; Vuister, G. W.; Zhu, G.; Pfeifer, J.; Bax, A. *J. Biomol. NMR* **1995**, *6*, 277.
(72) Johnson, B. A.; Blevins, R. A. *J. Biomol. NMR* **1994**, *4*, 603.